УДК 551.465

© *О. А. Атаджанова*[1], *А. В. Зимин*[1,2,3]
© Перевод *Е. С. Кочеткова*, 2019
[1] Институт океанологии им. П.П. Ширшова РАН, г. Москва
[2] Санкт-Петербургский государственный университет, г. Санкт-Петербург
[3] Институт водных проблем Севера Карельского научного центра РАН, г. Петрозаводск
oksana.atadzhanova@gmail.com

АНАЛИЗ ХАРАКТЕРИСТИК ПРОЯВЛЕНИЙ СУБМЕЗОМАСШТАБНЫХ ВИХРЕЙ БАРЕНЦЕВА, КАРСКОГО И БЕЛОГО МОРЕЙ ПО ДАННЫМ СПУТНИКОВЫХ НАБЛЮДЕНИЙ

Статья поступила в редакцию 23.01.2019, после доработки 08.07.2019

Приведены обобщенные результаты исследования поверхностных проявлений субмезомасштабных вихрей в Баренцевом, Карском и Белом морях на основе анализа около 3.5 тысяч спутниковых радиолокационных изображений в безледный период за несколько лет в период с 2007 по 2012 гг. Для выявления общих черт субмезомасштабной вихревой активности на фоне процессов большего масштаба использовались данные по температуре поверхности моря, по которым оценивалось положение фронтальных зон, и сведения о приливных процессах за тот же период.

На акваториях исследуемых морей было зарегистрировано около 4.5 тысяч структур. Показано, что субмезомасштабные вихри – распространенное явление в летний сезон на акватории описываемых морей. Чаще всего встречаются вихри диаметром 2–4 км. Установлено, что во всех морях преобладает циклонический тип проявлений вихрей, при этом размер антициклонических структур в среднем всегда больше. Максимальное число вихрей наблюдается в начальный период формирования сезонного приповерхностного пикноклина. Сопоставление положений поверхностных проявлений вихревых структур с положениями фронтальных зон и топографией дна показало, что частая встречаемость проявлений преимущественно отмечается вблизи и внутри областей изменчивости фронтальных зон, а также в районах со значительными неровностями дна. В районах подводных возвышенностей максимальное количество вихревых структур фиксировалось в период сизигийного прилива.

Ключевые слова: субмезомасштабные вихри, радиолокационные изображения, фронтальные зоны, прилив, Баренцево море, Карское море, Белое море.

O. A. Atadzhanova[1], *A. V. Zimin*[1,2,3]
[1] Shirshov Institute of Oceanology of Russian Academy of Sciences, Moscow
[2] St.-Petersburg State University, St.-Petersburg, Russia
[3] Northern Water Problems Institute, Karelian Research Centre, Russian Academy of Sciences, Petrozavodsk

ANALYSIS OF THE CHARACTERISTICS OF THE SUBMESOSCALE EDDY MANIFESTATIONS IN THE BARENTS, THE KARA AND THE WHITE SEAS USING SATELLITE DATA

Received 23.01.2019, in final form 08.07.2019

The paper presents generalized results of a study on submesoscale eddies' surface manifestations in the Barents, Kara, and White Seas based on the analysis of about 3.5 thousand satellite radar images during ice-free periods for several years from 2007 to 2012. For general features determination of submesoscale eddies' activity against processes of larger scale, sea surface temperature data, which allowed assessment of frontal zones position, and tidal data were used the same period. About 4.5 thousand structures were registered in the investigated seas. It is shown that submesoscale eddies are a common

Ссылка для цитирования: *Атаджанова О.А., Зимин А.В.* Анализ характеристик проявлений субмезомасштабных вихрей Баренцева, Карского и Белого морей по данным спутниковых наблюдений // Фундаментальная и прикладная гидрофизика. 2019. Т. 12, № 3. С. 36–45

For citation: *Atadzhanova O.A.*, *Zimin A.V.* Analysis of the characteristics of the submesoscale eddy manifestations in the Barents, the Kara and the White Seas using satellite data. *Fundamentalnaya i Prikladnaya Gidrofizika*. 2019, 12, 3, 36–45

DOI: 10.7868/S2073667319030055

phenomenon in the warm season in the areas of the Barents, Kara, and the White Seas. Eddy structures with a diameter from 2 to 4 km are most often registered. It has been established that the cyclonic type of eddies' manifestations is a prevalent type of structures, while the size of anticyclonic structures is larger on average. The maximum number of eddies is observed in the initial period of formation of the seasonal near-surface pycnocline. Comparison of the positions of eddies' surface manifestations, the frontal zone positions, and the bottom topography showed that the frequent occurrence of eddies is predominantly observed near and within the areas of the variability of the frontal zones. And also eddy structures are registered in regions where there are significant bottom irregularities. The maximum number of eddy structures in these regions was recorded principally during the period of a spring tide.

Keywords: submesoscale eddies, SAR-images, sea surface temperature, frontal zone, Barents Sea, Kara Sea, White Sea.

Introduction

Currently, submesoscale structures in different seas are studied arduously [1–10]. One of the principal data sources on these structures is the analysis of long-term satellite archives, which allows identification of where and when the manifestations of eddies are most often recorded. Studies [9, 11–13] have shown that submesoscale processes play an essential role in the intensification of mixing, horizontal, and vertical heat transfer.

However, available studies on separate water areas have not yet allowed the development of a general understanding of the submesoscale eddies' characteristics in the tidal Arctic seas (White, Barents, and Kara).

In this paper, submesoscale is defined as a short-period component of mesoscale with a spatial extent of the order of a few kilometers and a lifetime of up to several days. In this case, mesoscale structures, according to [14], are structures with a spatial extent from one to hundreds of kilometers and a lifetime from days to a season. The lower boundary of mesoscale, where the submesoscale is defined, equals to the baroclinic Rossby radius, which is determined, according to [15], for the Arctic basin in a range of one to a dozen of kilometers.

At this point, analysis of heterogeneous data for the White Sea (radar images (RI) for June–September 2009–2012, sea surface temperature (SST) for May–September 2010, in-situ temperature and salinity measurements for June–August 2006–2014) has showed that submesoscale eddy structures most frequently occur in the Dvina Bay and the Basin regions in the areas of fronts and continental slope; anticyclonic eddies are three times less frequent than cyclonic ones, but their diameters are overall larger; the average characteristics of the eddies vary only slightly from year to year during the same months; the maximum number of submesoscale eddies appear at the beginning of a warm season; near the Solovetsky Islands over the bottom irregularities (banks), the submesoscale eddies occur at a particular phase of the tide, they emerge in the upper 10–20 m layer and can be traced for 3–4 hours [16–18].

In the Barents Sea June–October 2007 and 2011 satellite data of RI and SST determined that areas of frequent eddy manifestations are frontal zones (according to 2007 data – up to 50%) and topography irregularities in the north-west of Franz Josef Land (FJL), near the eastern shore of the West Svalbard island, in the western part of the sea (in the area of the Atlantic waters), in the central part of the strait between the Russian Federal Nature Reserve and Novaya Zemlya, near the Kanin Nos Peninsula, and north of the Kola Peninsula; the most numerous manifestations emerge in July during, according to 2007 SST data, the most intense frontal dynamics; the predominant type of eddies' rotation is cyclonic, while the average diameter of such eddies is smaller than that of anticyclonic [18–19].

The peculiarities of submesoscale eddies for the Kara Sea were investigated with the RI data for June – October 2007. The data reveals that the most frequent eddies' manifestations emerge in the area of the Uyedineniya and Sverdrup (Pyasinsky Bay) islands, and also, near the western coast of the Yamal Peninsula, and south of the Cape Zhelaniya. Over 90% of the eddy structures present a cyclonic rotation type, and the average diameter of anticyclonic eddies is larger; the peak of eddies' activity was registered in August [18].

It is anticipated that in the Barents, Kara, and White Seas, one of the principal mechanisms for the eddy structures' formation can be the instability of currents in the areas of frontal zones and topographic effects resulting from flow over seamounts and depressions [13, 18, 21].

The geographical proximity of the seas, the similarities in characteristics and the spatial-temporal variability of the eddies' distribution, as well as possible mechanisms for their formation, formed the hypothesis basis: eddies' manifestation distribution generations have similar features in the tidal Arctic seas in focus. This hypothesis can be verified by a joint analysis of long-term archives of radar images using a single methodology in combination with the data on SST gradients, reflecting the dynamics of frontal zones (FZ), and bottom topography, and tides data.

The purpose of this work is to identify general features of the submesoscale eddies activity against the background of larger-scale processes (the formation of the seasonal pycnocline, averaged monthly and decadal frontal dynamics, tidal processes) in the Barents, Kara and White Seas according to radar images in the summer season.

Materials and methods

Radar images' arrays for the periods from June to October 2007 and 2011 were used as initial data to study the features of submesoscale eddies' surface manifestations across the Barents Sea (2007—1203 images, 2011—838 images), and across the Kara Sea (2007—900 images, 2011—275 images) acquired by ENVISAT ASAR in the C-band and WSM scanning modes (the track width is 400 × 400 km, the spatial resolution is 150 × 150 m) and IMP (100 × 100 km and 25 × 25 m, respectively). The average RI coverage was about 250 scenes per unit of water area over the Barents Sea and about 200 scenes per unit area across the Kara Sea. Over the White Sea, 221 radar images were analyzed covering May—September 2009—2012 (2009—60 images, 2010—111 images, 2011—37 images, and 2012—13 images) with an average coverage of 110 RI per unit of water area. Radar data covering 2009—2011 period was obtained with ENVISAT ASAR C-band in the same modes as for the Barents and Kara Seas, and in 2012, by satellites RADARSAT-1 with a spatial resolution of 25m in SGF scanning mode (Path Image) and RADARSAT-2 in the Fine Quad-Pol mode with a spatial resolution of 6 m. All satellite radar data were processed at the RSHU Satellite Oceanography Laboratory.

In radar images, eddy manifestations were detected as structures, which appeared in the form of dark and light stripes curved into spirals or arcs (examples of manifestations in fig. 1), and could also be inscribed in an ellipse. There are several mechanisms of eddy manifestations in radar images [22, 23]: film/slick (suppression of gravity-capillary waves by biogenic films), shear-wave (a combination of gravitational-capillary waves and shear flows), ice (tracer-ice). In this study, only those structures that were manifested in radar images using the first two mechanisms were considered. The coordinates of the center, the type of rotation (cyclonic/anticyclonic) and the diameter, which was calculated as the average between the lengths of the ellipse axes, were recorded. In more detail, the procedure for the determination of eddies is described in [24].

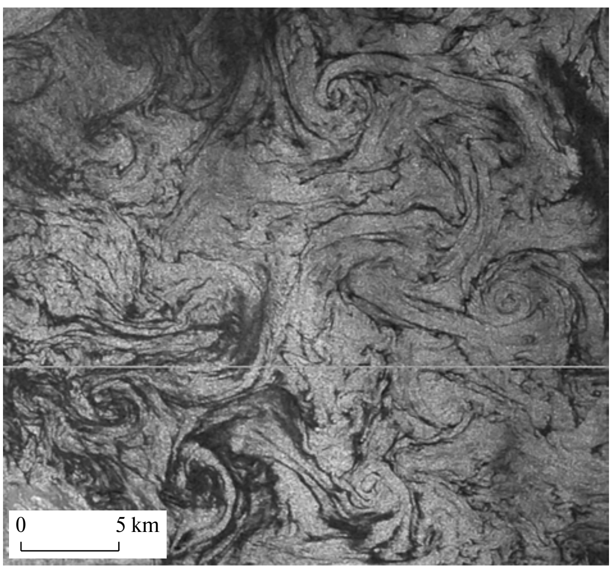

Fig. 1. Surface manifestations of eddy structures. Fragment of the radar image of the southwestern part of the Barents Sea (Envisat ASAR, WSM image mode, 09:10 UTC14.06.2007).

Рис. 1. Поверхностные проявления вихревых структур. Фрагмент радиолокационного изображения юго-западной части акватории Баренцева моря Envisat ASAR в режиме съемки WSM 09:10 UTC14.06.2007.

The frontal dynamics role in the Barents and Kara Seas was studied by the daily average SST data of the OSTIA GHRSST product. The daily SST data were averaged over decades and months, gradient fields were calculated with the same averaging periods. The areas of gradient maxima were identified according to the SST gradient maps, assigning a frontal zone (FZ) to an area where temperature gradient exceeded 0.02 °C/km were taken as the frontal zone (FZ). Within each FZ, a distinctive isotherm was selected that matches the main frontal section's location identified on the gradient map. The distinctive isotherm's location determined the edge of the main front inside the frontal zone for each decade and each month. The displacement of the decade average fronts and the FZ positions of over a month was taken as the region of the frontal zones variation, while the width of the frontal zones was estimated from three meridional sections of the SST gradient: 20°, 35° and 50° E for the Barents Sea and 65°, 75° and 80° E for the Kara Sea. For the White Sea, the average decade and monthly positions of the fronts obtained in [17] were used.

The role of frontal dynamics in the distribution of submesoscale eddies the analysis of composite maps were performed, which represented monthly the variability of FZ areas and locations of the eddies. The numbers of eddy manifestations within the variability areas were estimated, and the results are compiled in a summary table.

To identify the relationship between the positions of the eddies and tidal dynamics outside the areas of frontal variability, we analyzed the eddy structures of 2007 in areas with significant topography irregularities (over 10 m/km) in the Barents and Kara Seas (southwest of Franz Josef Land and northeast of the Uyedineniya island).

Results

In the framework of this study, the distribution of eddy structures manifestations in the Kara Sea during June–October 2011 was obtained for the first time. A total of 202 structures were registered. Comparison with previously available data on the eddies' manifestations obtained with radar images covering June–October 2007 [18] and showing 1242 structures, revealed multiple similarities in the spatial and temporal variability of the submesoscale eddies' features. The diameter varied from almost 1 km to 13–14 km, the difference between the average diameters for the season was 0.4 km (2.4 km in 2007, 2.8 km in 2011), while during both years the most common were eddies with diameters from 2 to 4 km (more than 50%). For these years, for both a month and a season as a whole, persisted the tendencies, such as cyclones prevailed over anticyclones (fig. 2, *a*) and that the average diameter of the anticyclones is larger.

However, the maximum recorded manifestations in each year were observed in different months – August (2007) and September (2011). This may be due to the difference in the coverage of radar data, ice conditions.

Comparison of two years' Kara Sea data with data on eddies in the Barents and White Seas allowed identification of common trends for the three seas in different years. Earlier [19], as a result of the analysis of radar images for June–October of 2007 and 2011, in the Barents Sea 2187 and 747 submesoscale eddy structures with a diameter from 0.2 km to 25 km were registered. The peak of the eddy activity for both the season in general (fig. 2, *b*) and each year was observed in July, with up to a half of the eddies measuring from 2 to 4 km, the average monthly diameter during the season varied from 2.3 to 4.2 km. In the White Sea, during May–September 2009–2012, 162 manifestations of submesoscale eddies with a diameter from 0.9 km to 13.2 km were recorded [16, 18]. The most frequent observations of eddies befell on July with the variability of the monthly average diameter from 2.2 km to 5.1 km. Albeit, the abundance of eddies with diameter from 2 to 4 km, at least 75% of the detected eddies had a scale comparable with the baroclinic Rossby radius, concurrently, the eddies' predominance (above 80% instances) of a cyclonic rotation was discerned, which is ordinary for each month (fig. 2, *c*).

The average spatial dimensions of the detected eddy structures in each of the three studied seas over the entire period had a scale of the baroclinic Rossby radius, which average values are 4.9 km for the Barents Sea,

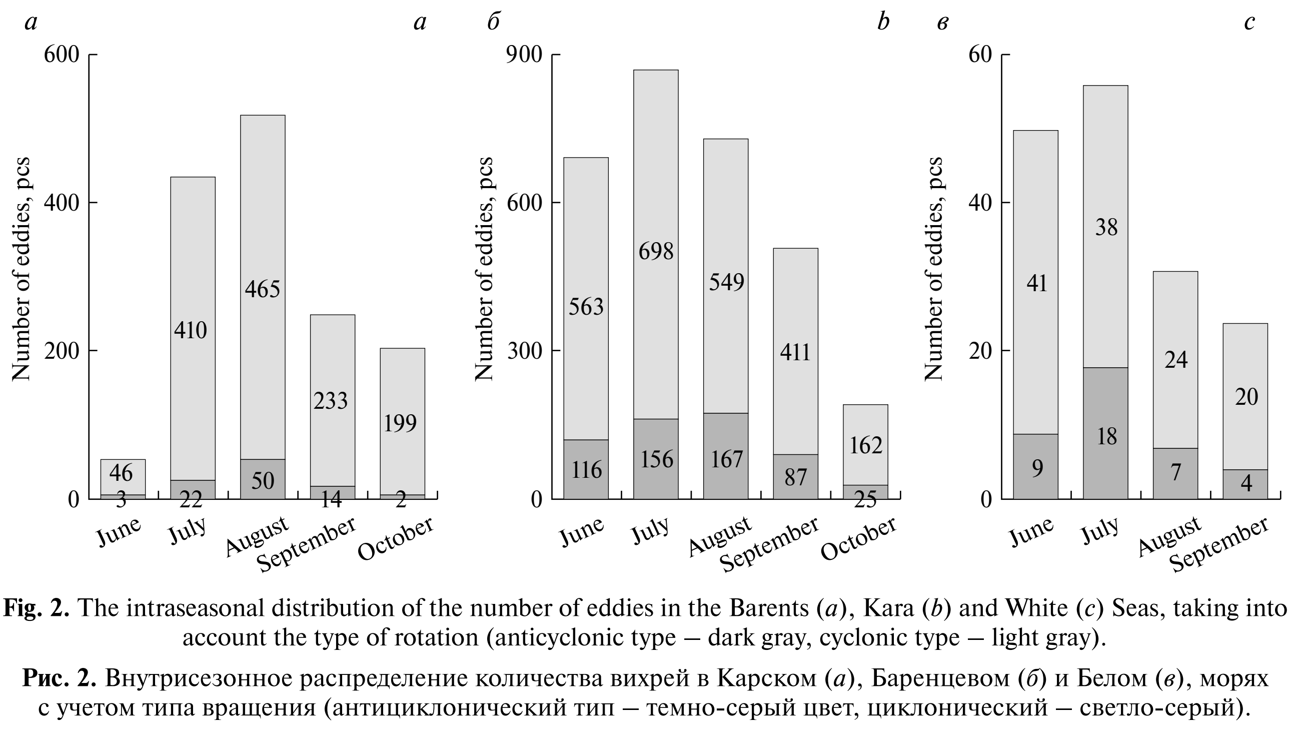

Fig. 2. The intraseasonal distribution of the number of eddies in the Barents (*a*), Kara (*b*) and White (*c*) Seas, taking into account the type of rotation (anticyclonic type – dark gray, cyclonic type – light gray).

Рис. 2. Внутрисезонное распределение количества вихрей в Карском (*а*), Баренцевом (*б*) и Белом (*в*), морях с учетом типа вращения (антициклонический тип – темно-серый цвет, циклонический – светло-серый).

3 km for the Kara Sea, and 4.3 km for the White Sea [18]. Aforementioned suggests that the necessary condition for the baroclinic instability existence is fulfilled [20]; namely, the square of the ratio of the baroclinic Rossby radius R to the scale of disturbances L (eddy structure) must be less than or of the order of unity. Hence follows that for eddy structures with a spatial scale (diameter) of an order or exceeding the baroclinic Rossby radius one of the formation drivers can be baroclinic instability, which is usually observed in the areas of the frontal zones.

In all the seas, the fronts and FZs in the SST were most clearly manifested from June to September. In the White Sea, several major FZs are present [25]: two frontal zones of runoff genesis in the Dvina and Onega bays, and two shelf-tidal FZs in the Gorlo Strait and around the Solovki islands. The width of the FZs in the White Sea ranged from 10 to 140 km [13]. Despite the marginal dynamics of the average monthly positions of the fronts, the average decade positions of the fronts showed a significant shift during almost every studied month.

In the Barents Sea, the Arctic Marginal Ice and Polar frontal zones were recorded. The former is associated with the ice melting and located in the northern part of the sea [21], following from the Spitsbergen archipelago to the border of the Kara Sea. The latter, Polar FZ is located in the central part of the Barents Sea [26] and presents the boundary between the Barents Sea and Atlantic waters and extends from the southern tip of the Svalbard archipelago through the entire sea to its southeast part. The width of the FZ in the Barents Sea ranged from 70 to 180 km. The main front of the Arctic Marginal Ice frontal zone during the summer season moved across the whole northern part of the Barents Sea. It was most dynamic in July and reached the northernmost position in August in both years. The main front of the Polar FZ appeared quasi-stationary in the western side of the sea, and in the eastern side from June to August it advanced towards the Novaya Zemlya archipelago, while the most intense front dynamics observed in 2007.

The Arctic Marginal Ice and River Plums frontal zones [27–29] are identified in the Kara Sea. The Arctic Marginal Ice frontal zone has similar genesis to the above-described FZ in the Barents Sea. The River Plums FZ is the boundary between the Kara Sea waters and the modified freshwater continental runoff and located southeast of the Novaya Zemlya archipelago in the central and southwestern sectors of the sea. In the Kara Sea, the width of the frontal zones ranged from 70 to 150 km. In both years, the northernmost position of the main front of the Arctic Marginal Ice FZ was observed in August, while it was most dynamic in 2007. The main front of the River Plums FZ moved predominantly in the northern and western directions towards Novaya Zemlya. In 2007 the front approached Novaya Zemlya in July and split into two parts, nevertheless the northern part was not detected in September. In 2011, the main front of the River Plums FZ was fully observed only in July, while it was closer to Novaya Zemlya than in 2007. However, in August and September, it was possible to register only its northern part, near the northern tip of Novaya Zemlya.

All fronts experienced the greatest displacements of tens and hundreds of kilometers per month in the first half of the summer season under the influence of, obviously, synoptic processes and intense freshwater runoff against the background of insufficient heating of the upper layer, but their high dynamic activity persisted and later, manifesting itself as the formation of tongues and meanders sizes up to several tens of kilometers. In all seas, the maximum variability of the positions of the FZ is observed in July. The dynamics of the fronts, the FZs, and the variability of their characteristics are described in more detail in different papers [13, 17, 30, 31].

Figure 3 (see Insert) shows an example of a comparison of the SST gradient field averaged over the first decade of July 2007 and the positions of the eddy structures' centers in the same period for the region southeast of the Svalbard archipelago. It can be seen that most of the manifestations of eddy structures are observed inside and near zones of the increased temperature gradient (more than 0.2 °C/km), which are associated with the FZ. The similar picture is characteristic for all considered seas.

For the first time, the number of eddy structures' manifestations was estimated within the regions of the decadal variability of the fronts in the Kara Sea in July – September 2007 and 2011, and a comparison was made with similar estimates for the Barents [19] and White Seas [17].

In the Kara Sea, eddies within the variability regions were registered every month (table) during the periods in which the possibility of detecting the fronts' position existed. For July–September 2007 and 2011 within the regions of variability, 23%, and 39% of the total number of the eddies were recorded, respectively. The manifestations were observed in both years most often in July, 27% in 2007 and 64% in 2011 when the variability regions were the most expansive and pycnocline was close to the surface. The least amount of eddies within these regions in 2007 was observed in September (13%), and in 2011 – in August (17%).

The months of maximum and a minimum number of manifestations within the variability areas overall coincide in both the Barents and the White Seas [17, 19]. In the Barents Sea in 2007 and 2011 within the fronts' variability areas, 23% and 30% of all eddies were recorded, respectively (table). The least number of manifestations was reported in each year in September (10% each) when the frontal dynamics was insignificant compared to other months. Most of the eddies were observed within the regions of the FZ variability in July (38% and 49% in 2007 and 2011, respectively). This month was distinguished by the most intense intramonthal frontal dynamics, expressed in a significant change in the position of the fronts over the decades, and the near-surface seasonal pycnocline formation occurred.

In the White Sea in each month, except for September (13%), more than 50% of the eddies identified on the sea surface belonged to the regions. At the same time, the maximum, both in the Barents and Kara Seas, was observed in July – 77%, when the most intense decadal displacement of fronts was registered, the seasonal pycnocline only started to develop and was still close to the surface.

The above suggests that in all three seas, there is a connection between the frequency of eddy structures manifestations and frontal dynamics, which contributes to the development of processes associated with barocline instability.

Table

The number of eddies within the areas of variability of the frontal zones as a percentage of the number of registered eddies for each month

Количество вихрей внутри областей изменчивости фронтальных зон в процентах от количества зарегистрированных вихрей за каждый месяц

Month	Barents Sea		Kara Sea		White Sea
	2007	2011	2007	2011	2010
June	24	23	–	–	62
July	38	49	27	64	77
August	13	30	23	17	57
September	10	10	13	29	13
Total	23	30	23	39	57

Except for the frontal zones' areas, the eddy manifestations were repeatedly registered in the areas of the seabed elevations. In the previous work on the White Sea [13], contact observations over several years confirmed that the eddies' formation in the areas of the seafloor elevations is associated with tidal dynamics. According to the radar data, such areas are located north of the Solovetsky Islands and near the Tersky coast, where significant differences in depths are present.

In this study, for the first time, an attempt was made to find a relationship between the positions of eddy manifestations and topographic effects, as the cause of the formation of eddy structures in areas of topographic irregularities under the influence of tidal dynamics in the Barents and Kara Seas.

RI data analysis revealed that in these seas, eddies are registered frequently in the areas above seabed irregularities. In the Barents Sea, these areas are mostly attributed to the northern sector, and in the Kara Sea – to the central and northern sectors. Meanwhile, the eddies were registered in these areas throughout practically the entire studied period, when these areas were free of ice. The eddies' positions and topographic effects relationship was studied with the parameters of eddy structures' manifestations upon the 2007 data in the region south-west of the FJL (from June to October), and northeast of the Uyedineniya Island (from August to October). As an example, the distribution of eddy structures on the seafloor relief map in the selected area of the Barents Sea is shown in fig. 4 (see Insert). Eddy structures in the studied areas were registered every month during no-ice periods, regardless of the frontal zones' position, which facilitated their identification. The characteristics of the observed eddies in the studied areas were close to the average values for each sea.

From June to October, 171 eddy manifestations were registered south-west of Franz Josef Land; anticyclonic eddies were almost six times more frequent than cyclonic. The monthly average diameter for the season of 2007 was 3 km. Northeast of the Uyedineniya island, eddies were observed only from August to October as in June and July the area was covered with ice. A total of 24 manifestations were registered. Cyclonic rotation eddies were seven times more numerous than anticyclonic. The average monthly diameter in the study area was 2 km.

In the regions (Cape Flora (Barents Sea) and the Wiese Island (Kara Sea)), comparison of the time of the eddy structures emergence with tide data showed that the eddies were most often observed during the spring tide period during the most rapid tidal currents. For the region southwest of the Franz Josef Land, during spring tide the number of eddies amounted to more than 55%, while in the quadrature tide it was 20%. In the region northeast of the Uyedineniya Island, more than 90% of the manifestations were recorded during the syzygy and only 4% during the quadrature.

The registration of surface manifestations of eddy structures above the irregularities of the seafloor predominantly during the period of spring tide currents (when tidal velocities are maximal) suggests that the formation of eddies in these areas is associated with the intensity of tidal currents.

Conclusion

For the first time, the analysis of more than 250 radar images for June–October 2011 for the Kara Sea on the eddy structures' manifestations, and the subsequent comparison of the results with the data on eddy manifestations for periods: June–October 2007 in the Kara Sea, June–October 2007, and 2011 – the Barents Sea, and May–September 2009–2012 – the White Sea, made it possible to identify general trends in the distribution of submesoscale eddies' manifestations in the tidal Arctic seas.

Based on the comparison of the spatial-temporal distribution of the described manifestations, similar features were identified in the intraseasonal variability of the eddies' characteristics, which are generally repeated for each year, and shred by each of the three seas. It was discovered that the predominant direction of eddies' rotation was cyclonic (at least 75% of the registered cases), while the size of the anticyclonic eddies was on average larger by 20%. Eddies with a diameter of 2 to 4 km (~45% of the manifestations in the Barents, ~55% in the Kara, ~40% in the White Seas) were recorded most frequently, and the most intense eddy activity was observed during the formation of the near-surface pycnocline (early summer).

It was shown for the first time that for most of the registered eddies in each of the three seas, the condition of baroclinic instability is satisfied, which allows, but does not prove, that it can be a generation mechanism in the areas of the frontal zones.

The estimates comparison of the number of eddies within the regions of the variability of the decade-average fronts also showed a general behaviour that was observed in July in each of the three seas. The greatest monthly number of eddies within the regions of frontal zones variability was recorded in each of the seas every of the studied years in July: up to 49% in the Barents Sea, up to 64% in the Kara Sea, and up to 77% in the White Sea during intense frontal dynamics. With all that, in the Barents and Kara Seas, the frequent occurrence regions repeated from year to year. Thus, it appears that under conditions of a shallow and sharp pycnocline in the FZ area, frontal dynamics processes can make a significant contribution to the generation of eddy structures. The genesis of most submesoscale eddies is associated with disturbances in the position and the characteristics of the fronts under the influence of structure-forming processes of various origins.

In the areas with seafloor irregularities, eddy structures were registered when these areas appeared free of ice and mainly during the period of maximum tidal current velocities (spring tide). That emphasizes the role of the tide, which is a significant factor in the formation of not only mesoscale variability but the processes of eddy formation.

The patterns revealed in the process of the comparison of the eddies' characteristics demonstrate a commonality in the distribution of submesoscale eddies' manifestations in the waters of the Barents, Kara, and White Seas. It seems that eddies with a spatial size of the order from one to a dozen kilometers with a cyclonic type of rotation, occurring mainly in the period of pycnocline formation, in the vicinity of frontal areas and seabed irregularities are typical structural elements of the Arctic seas' dynamics.

The authors thank Kozlov I.E. for providing radar images, Konik A.A. and Svergun E.I. for their help in processing satellite data, Romanenkov D.A. for participating in the discussion of the results of the work.

The processing of radar images and their analysis in order to identify the eddy structures was carried out within the framework of the Russian Foundation of Basic Research grant No. 18-35-20078 mol_a_ved "Meso- and submesoscale dynamics of the upper Arctic Ocean: synthesis of satellite observations, contact measurements and numerical simulation results". Data processing on the sea surface temperature in order to identify the fronts and a joint analysis of the eddies' structures distribution, the fronts position, bottom topography and tidal features were carried out as part of the government assignment on the project number 0149-2019-0015 "Wave processes, transport phenomena and biogeochemical cycles in the seas and oceans: a study of formative mechanisms based on physico-mathematical modeling and full-scale experimental work".

Литература

1. *Mahadevan A.*, *Tandon A.* An analysis of mechanisms for submesoscale vertical motion at ocean fronts // Ocean Modell. 2006. V. 14. P. 241–256.
2. *Thomas L.N.*, *Tandon A.*, *Mahadevan A.* Submesoscale processes and dynamics // Ocean Modeling in an Eddying Regime, Geophys. Monogr. Ser. 2008. V. 177. P. 17–38.
3. *Костяной А.Г.*, *Гинзбург А.И.*, *Шеремент Н.А.*, *Лаврова О.Ю.*, *Митягина М.И.* Мелкомасштабные вихри Черного моря // Современные проблемы дистанционного зондирования Земли из космоса. 2010. Т. 7, № 1. С. 248–259.
4. *Зацепин А.Г.*, *Баранов В.И.*, *Кондрашов А.А.*, *Корж А.О.*, *Кременецкий В.В.*, *Островский А.Г.*, *Соловьев Д.М.* Субмезомасштабные вихри на Кавказском шельфе Черного моря и порождающие их механизмы // Океанология. 2011. Т. 51, № 4. С. 592–605.
5. *Митягина М.И.*, *Лаврова О.Ю.* Спутниковые наблюдения вихревых и волновых процессов в прибрежной зоне северо-восточной части Черного моря // Исследование Земли из космоса. 2009. № 5. С. 72–79.
6. *Каримова С.С.* Статистический анализ субмезомасштабных вихрей Балтийского, Черного и Каспийского морей по данным спутниковой радиолокации // Исследование Земли из космоса. 2012. № 3. С. 31–47.
7. *Karimova S.*, *Gade M.* Eddies in the Red Sea as seen by satellite SAR imagery // Remote Sensing of the African Seas. Berlin Heidelberg: Springer-Verlag, 2014. P. 357–378.
8. *Redondo J.M.*, *Karimova S.S.* Eddy structure and patterns in the oceans and atmospheres // In Proceedings Topical Problems of Fluid Mechanics, Prague, 2018. P. 235–242.
9. *Mensa J.A.*, *Timmermans M.-L.*, *Kozlov I.E.*, *Williams W.J.*, *Özgökmen T.* Surface drifter observations from the Arctic Ocean's Beaufort Sea: Evidence for submesoscale dynamic // Journal of Geophysical Research: Oceans. 2018. V. 123. P. 2635–2645.
10. *Костяной А.Г.*, *Гинзбург А.И.*, *Лаврова О.Ю.*, *Митягина М.И.* Дистанционное зондирование субмезомасштабных вихрей в морях России // Сборник трудов Международного симпозиума «Мезомасштабные и субмезомасштабные процессы в гидросфере и атмосфере» (МСП-2018), посвященного 90-летию проф. К.Н. Федорова. М.: ИО РАН, 2018. С. 184–187.
11. *Zhao M.*, *Timmermans M.-L.*, *Cole S.*, *Krishfield R.*, *Proshutinsky A.*, *Toole J.* Characterizing the eddy field in the Arctic Ocean halocline // Journal of Geophysical Research Oceans. 2014. V. 119, № 12. P. 8800–8817.
12. *Manucharyan G.E.*, *Thompson A.F.* Submesoscale sea ice-ocean interactions in marginal ice zones // Journal of Geophysical Research: Oceans. 2017. V. 122, № 12. P. 9455–9475.
13. *Зимин А.В.* Субприливные процессы и явления в Белом море. М: ГЕОС, 2018. 220 с.
14. *Dickey T.D.*, *Lewis M.R.*, *Chang G.C.* Optical oceanography: recent advances and future directions using global remote sensing and in situ observations // Reviews of Geophysics. 2006. V. 44(1). P. 1–39.
15. *Nurser A.J. G.*, *Bacon S.* The Rossby radius in the Arctic Ocean // Ocean Science. 2014. V. 10, № 6. P. 967–975.
16. *Зимин А.В.*, *Атаджанова О.А.*, *Романенков Д.А.*, *Козлов И.Е.*, *Шапрон Б.* Субмезомасштабные вихри в Белом море по данным спутниковых радиолокационных измерений // Исслед. Земли из космоса. 2016. № 1–2. С. 129–135.
17. *Романенков Д.А.*, *Зимин А.В.*, *Родионов А.А.*, *Атаджанова О.А.*, *Козлов И.Е.* Изменчивость фронтальных разделов и особенности мезомасштабной динамики вод Белого моря // Фундаментальная и прикладная гидрофизика. 2016. Т. 9, № 1. С. 59–72.
18. *Атаджанова О.А.*, *Зимин А.В.*, *Романенков Д.А.*, *Козлов И.Е.* Наблюдение малых вихрей в Белом, Баренцевом и Карском морях по данным спутниковых радиолокационных измерений // Морской гидрофизический журнал. 2017. № 2. С. 80–90.
19. *Атаджанова О.А.*, *Зимин А.В.*, *Свергун Е.И.*, *Коник А.А.* Субмезомасштабные вихревые структуры и фронтальная динамика в Баренцевом море // Морской гидрофизический журнал. 2018. № 3. С. 237–246.
20. *Каменкович В.М.*, *Кошляков М.М.*, *Монин А.С.* Синоптические вихри в океане. Л.: Гидрометеоиздат, 1987. 511 с.
21. *Родионов В.Б.*, *Костяной А.Г.* Океанические фронты морей Северо-европейского бассейна. М.: ГЕОС, 1998. 292 с.
22. *Каримова С.С.* О проявлении вихревых структур на радиолокационных изображениях // Современные проблемы дистанционного зондирования Земли из космоса. 2010. Т. 7, № 3. С. 152–160.
23. *Karimova S.* Spiral eddies in the Baltic, Black and Caspian seas as seen by satellite radar data // Advances in Space Research. 2012. V. 50. P. 1107–1124.
24. *Атаджанова О.А.* Особенности субмезомасштабной вихревой динамики Баренцева, Карского и Белого морей по данным спутниковых наблюдений: дис. ... канд. геогр. наук: 25.00.28. ИО РАН, СПб., 2019. 135 с.
25. *Пантюлин А.Н.* Динамика, структура и водные массы: глава в монографии «Система Белого моря. Том II. Водная толща и взаимодействующая с ней атмосфера, криосфера, речной сток и биосфера». М.: Научный мир, 2012. С. 309–379.
26. *Vage S.*, *Basedow S.L.*, *Tande K.S.*, *Zhou M.* Physical structure of the Barents Sea Polar Front near Storbanken in August 2007 // Journal of Marine System. 2014. V. 130. P. 256–262.

27. *Pavlov V.K.*, *Timokhov L.A.*, *Baskakov G.A.*, *Kulakov M.Y.*, *Kurazhov V.K.*, *Pavlov P.V.*, *Pivovarov S.V.*, *Stanovoy V.V.* Hydrometeorological regime of the Kara, Laptev, and EastSiberian seas / Technical Memorandum APL–UW TM1–96, University of Washington, 1996. 179 p.
28. *Кубряков А.А.*, *Станичный С.В.*, *Зацепин А.Г.*, *Кременецкий В.В.* Распространение речных вод в Черном и Карском морях по спутниковым измерениям уровня, солености и хлорофилла А // Экологическая безопасность прибрежной и шельфовой зон и комплексное использование ресурсов шельфа. Севастополь: МГИ НАНУ, 2013. № 27. С. 394–398.
29. *Сергеева В.М.*, *Суханова И.Н.*, *Дружкова Е.И.*, *Сажин А.Ф.*, *Демидов А.Б.*, *Мошаров С.А.*, *Кременецкий В.В.*, *Полухин А.С.* Структура и распределение фитопланктона в глубоководных районах северной части Карского моря // Экосистема Карского моря – новые данные экспедиционных исследований. Материалы научной конференции. М.: АПР, 2015. С. 111–115.
30. *Зимин А.В.*, *Коник А.А.*, *Атаджанова О.А.* Количественные оценки изменчивости характеристик температуры поверхности моря в районе фронтальных зон Баренцева моря // Ученые записки Российского государственного гидрометеорологического университета. 2018. № 51. С. 99–108.
31. *Коник А.А.*, *Атаджанова О.А.*, *Зимин А.В.* Фронтальные зоны Баренцева и Карского морей // Процессы в геосредах. № 3(17). 2018. С. 239–240.

References

1. *Mahadevan A.*, *Tandon A.* An analysis of mechanisms for submesoscale vertical motion at ocean fronts. *Ocean Modell.* 2006, 14, 241–256.
2. *Thomas L.N.*, *Tandon A.*, *Mahadevan A.* Submesoscale processes and dynamics. *Ocean Modeling in an Eddying Regime*, *Geophys. Monogr. Ser.* 2008, 177, 17–38.
3. *Kostyanoj A.G.*, *Ginzburg A.I.*, *Sherement N.A.*, *Lavrova O.Yu.*, *Mityagina M.I.* Small-scale eddies in the Black Sea. *Sovremennye Problemy Distancionnogo Zondirovaniya Zemli iz Kosmosa*. 2010, 7(1), 248–259 (in Russian).
4. *Zatsepin A.G.*, *Kremenetskiy V.V.*, *Ostrovskii A.G.*, *Baranov V.I.*, *Kondrashov A.A.*, *Korzh A.O.*, *Soloviev D.M.* Submesoscale eddies at the caucasus Black Sea shelf and the mechanisms of their generation. *Oceanology.* 2011, 51, 4, 554–567.
5. *Mityagina M.I.*, *Lavrova O.Yu.* Satellite observations of eddy and wave processes in the coastal waters of the North-Eastern Black Sea. *Issledovanie Zemli iz Kosmosa*. 2009, 5, 72–79 (in Russian).
6. *Karimova S.S.* Statistical analysis of submesoscale eddies in the Baltic, Black and Caspian Seas using satellite SAR images. *Issledovanie Zemli iz Kosmosa*. 2012, 3, 31–47 (in Russian).
7. *Karimova S.*, *Gade M.* Eddies in the Red Sea as seen by satellite SAR imagery. *Remote Sensing of the African Seas. Berlin Heidelberg: Springer-Verlag*, 2014, 357–378.
8. *Redondo J.M.*, *Karimova S.S.* Eddy structure and patterns in the oceans and atmospheres. *Proceedings Topical Problems of Fluid Mechanics*, *Prague.* 2018, 235–242.
9. *Mensa J.A.*, *Timmermans M.-L.*, *Kozlov I.E.*, *Williams W.J.*, *Özgökmen T.* Surface drifter observations from the Arctic Ocean's Beaufort Sea: Evidence for submesoscale dynamic. *Journal of Geophysical Research: Oceans.* 2018, 123, 2635–2645.
10. *Kostyanoj A.G.*, *Ginburg A.I.*, *Lavrova O.Yu.*, *Mityagina M.I.* Remote sensing of submesoscale eddies in the seas of Russia. *Sbornik trudov Mezhdunarodnogo simpoziuma «Mezomasshtabnye i submezomasshtabnye processy v gidrosfere i atmosfere» (MSP-2018)*, *posvyashhennogo 90-letiyu prof. K.N. Fedorova. M.*: *IO RAN*, 2018, 184–187 (in Russian).
11. *Zhao M.*, *Timmermans M.-L.*, *Cole S.*, *Krishfield R.*, *Proshutinsky A.*, *Toole J.* Characterizing the eddy field in the Arctic Ocean halocline. *Journal of Geophysical Research Oceans.* 2014, 119, 12, 8800–8817.
12. *Manucharyan G.E.*, *Thompson A.F.* Submesoscale sea ice-ocean interactions in marginal ice zones. *Journal of Geophysical Research: Oceans.* 2017, 122, 12, 9455–9475.
13. *Zimin A.V.* Subtidal processes and phenomena in the White Sea. M., GEOS, 2018. 220 p (in Russian).
14. *Dickey T.D.*, *Lewis M.R.*, *Chang G.C.* Optical oceanography: recent advances and future directions using global remote sensing and in situ observations. Reviews of Geophysics. 2006, 44, 1, 1–39.
15. *Nurser A.J.G.*, *Bacon S.* The Rossby radius in the Arctic Ocean. Ocean Science. 2014, 10, 6, 967–975.
16. *Zimin A.V.*, *Atadzhanova O.A.*, *Romanenkov D.A.*, *Kozlov I.E.*, *Shapron B.* Submesoscale eddies in the White Sea based on satellite SAR data. *Issled. Zemli iz Kosmosa*. 2016, 1–2, 129–135 (in Russian).
17. *Romanenkov D.A.*, *Zimin A.V.*, *Rodionov A.A.*, *Atadzhanova O.A.*, *Kozlov I.E.* Variability of Fronts and Features of Mesoscale Water Dynamics in the White Sea. *Fundamentalnaya i Prikladnaya Gidrofizika*. 2016, 9 (1), 59–72 (in Russian).
18. *Atadzhanova O.A.*, *Zimin A.V.*, *Romanenkov D.A.*, *Kozlov I.E.* Satellite radar observations of small eddies in the White, Barents and Kara Seas. *Physical Oceanography*. 2017, 2, 75–83.
19. *Atadzhanova O.A.*, *Zimin A.V.*, *Svergun E.I.*, *Konik A.A.* Submesoscale Eddy Structures and Frontal Dynamics in the Barents Sea. *Physical Oceanography.* 2018, 3, 220–228.

20. *Kamenkovich V.M.*, *Koshlyakov M.M.*, *Monin A.S.* Synoptic eddies in the ocean. *L.*, *Gidrometeoizdat*, 1987, 511 p. (in Russian).
21. *Rodionov V.B.*, *Kostyanoj A.G.* Ocean fronts of the seas of the North European basin. *M.*, *GEOS*, 1998, 292 p. (in Russian).
22. *Karimova S.S.* About vortical structures manifestation in satellite radar images. *Sovremennye Problemy Distantsionnogo Zondirovaniya Zemli iz Kosmosa*. 2010, 7, 3, 152–160 (in Russian).
23. *Karimova S.* Spiral eddies in the Baltic, Black and Caspian seas as seen by satellite radar data. *Advances in Space Research*. 2012, 50, 1107–1124.
24. *Atadzhanova O.A.* Features of the submesoscale eddy dynamics of the Barents, Kara and White Seas according to satellite observations: dis. ... kand. geogr. nauk: 25.00.28. *IO RAN*, *SPb.*, 2019. 135 p. (in Russian).
25. *Pantyulin A.N.* Dynamics, structure and water masses. The system of the White Sea. Volume II The water column and the atmosphere interacting with it, the cryosphere, river runoff and biosphere. *M.*, *Nauchnyj mir*, 2012, 309–379 (in Russian).
26. *Vage S.*, *Basedow S.L.*, *Tande K.S.*, *Zhou M.* Physical structure of the Barents Sea Polar Front near Storbanken in August 2007. *Journal of Marine System*. 2014, 130, 256–262.
27. *Pavlov V.K.*, *Timokhov L.A.*, *Baskakov G.A.*, *Kulakov M.Y.*, *Kurazhov V.K.*, *Pavlov P.V.*, *Pivovarov S.V.*, *Stanovoy V.V.* Hydrometeorological regime of the Kara, Laptev, and EastSiberian seas. *Technical Memorandum APL–UW TM1–96*, *University of Washington*, 1996. 179 p.
28. *Kubryakov A.A.*, *Stanichnyj S.V.*, *Zacepin A.G.*, *Kremeneckij V.V.* The propagation of the river waters in the Black and Kara sea from satellite measurements of sea level, salinity and concentration of the chlorophylla a. *E'kologicheskaya bezopasnost' pribrezhnoj i shel'fovoj zon i kompleksnoe ispol'zovanie resursov shel'fa. Sevastopol'*, *MGI NANU*, 2013, 27, 394–398 (in Russian).
29. *Sergeeva V.M.*, *Suxanova I.N.*, *Druzhkova E.I.*, *Sazhin A.F.*, *Demidov A.B.*, *Mosharov S.A.*, *Kremeneckij V.V.*, *Poluxin A.S.* The structure and distribution of phytoplankton in the deep waters of the northern Kara Sea. *E'kosistema Karskogo morya – novye dannye e'kspedicionnyx issledovanij. Materialy nauchnoj konferencii. M.*, *APR*, 2015, 111–115 (in Russian).
30. *Zimin A.V.*, *Konik A.A.*, *Atadzhanova O.A.* Quantitative estimations of the variability of characteristics of the temperature of the sea (SST) surface in the front of the frontal zone of the Barents Sea. *Uchenye Zapiski Rossijskogo Gosudarstvennogo Gidrometeorologicheskogo Universiteta*. 2018, 51, 99–108 (in Russian).
31. *Konik A.A.*, *Atadzhanova O.A.*, *Zimin A.V.* Frontal zones of the Barents and Kara Seas. *Processy v Geosredakh*. 2018, 3(17), 239–240 (in Russian).

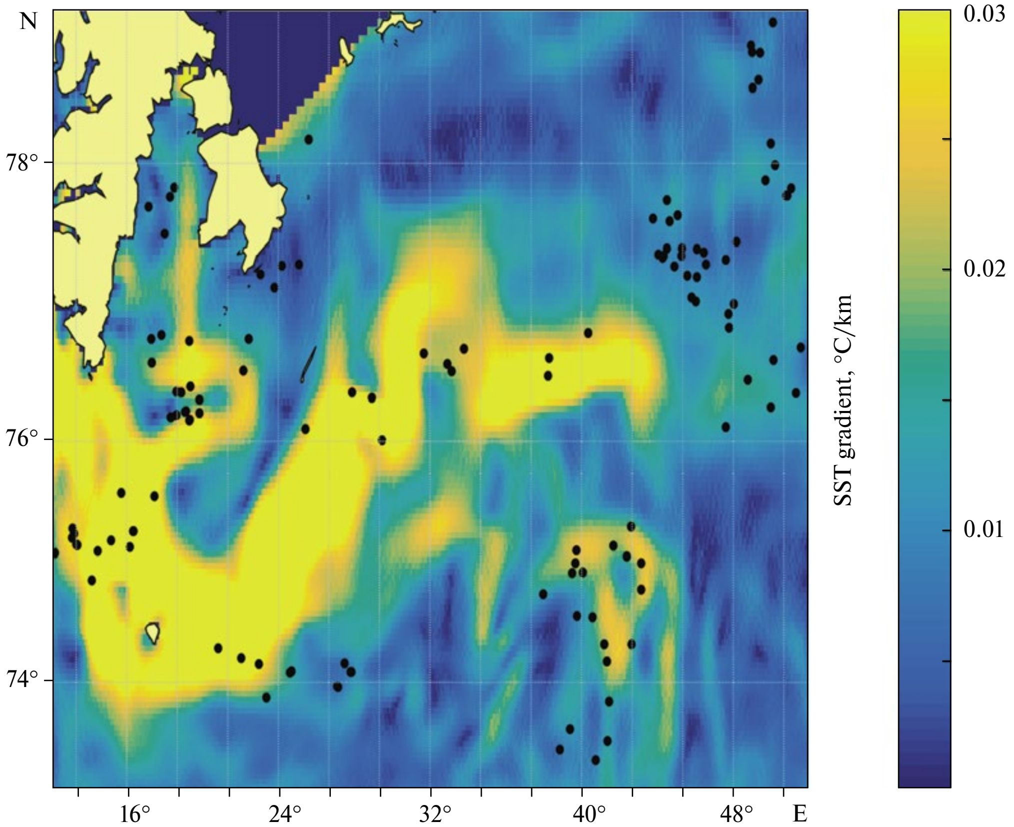

Fig. 3. Map of the average decade values of the SST gradient for the 1st decade of July, 2007. The black dots on the map show the center positions of manifestations of submesoscale eddies according to the radar images for the same period.

Рис. 3. Карта среднедекадных значений градиента ТПМ за 1 декаду июля 2007 г. Черными точками на карте показаны положения центров проявлений субмезомасштабных вихрей по данным РЛИ за тот же период.

К статье *Атаджанова О. А., Зимин А. В.* Анализ характеристик проявлений...

Atadzhanova O. A., Zimin A. V. Analysis of the characteristics of the submesoscale...

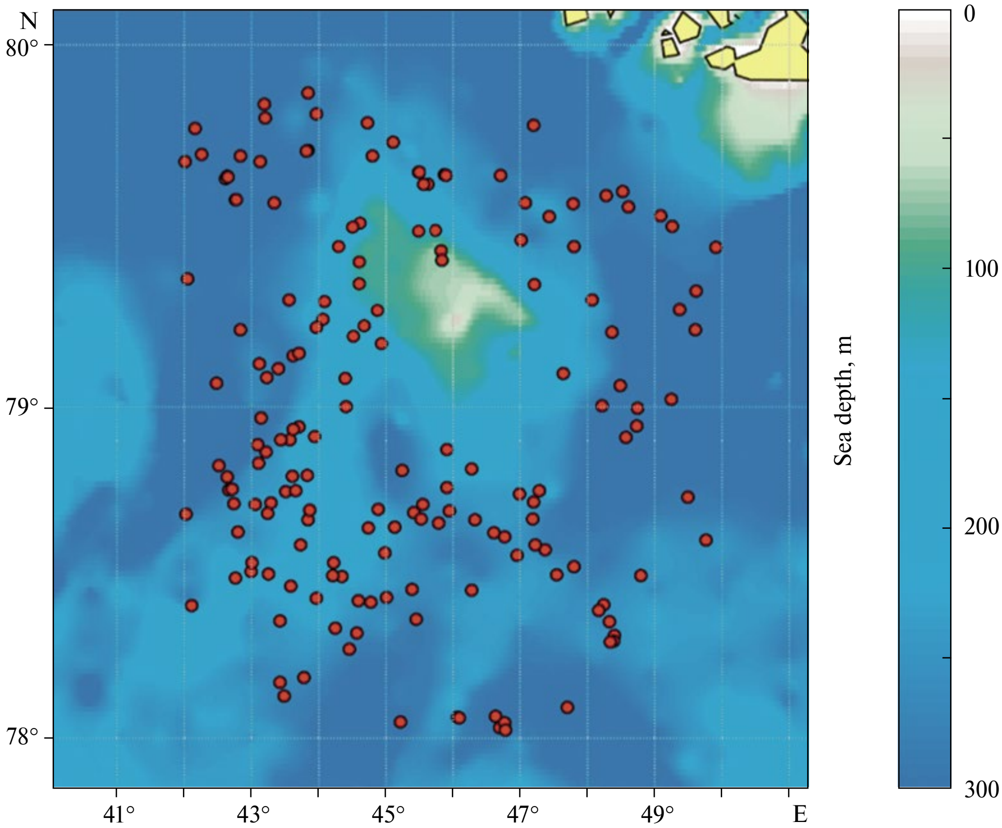

Fig. 4. Map of the depths of the region southwest of Franz Josef Land in the Barents Sea, where red dots indicate the center positions of the eddies during the warm season of 2007.

Рис. 4. Карта глубин района юго-западнее ЗФИ в Баренцевом море, где красными точками обозначены положения центров вихрей за июнь – октябрь 2007 г.